# Supporting Information

# 3D-RISM-MP2 Approach to Hydration Structure of Pt(II) and Pd(II) Complexes: Unusual H-Ahead Mode vs. Usual O-Ahead One

Shinji Aono,[†] Toshifumi Mori,[‡] and Shigeyoshi Sakaki[*,†]

*Fukui Institute for Fundamental Chemistry, Kyoto University, Nishihiraki-cho, Takano, Sakyo-ku, Kyoto 606-8103, Japan, and Institute for Molecular Science, Okazaki, Aichi 444-8585, Japan and School of Physical Sciences, The Graduate University for Advanced Studies, Okazaki, Aichi 444-8585, Japan*

E-mail: sakaki.shigeyoshi.47e@st.kyoto-u.ac.jp

[*]To whom correspondence should be addressed

[†]Fukui Institute for Fundamental Chemistry, Kyoto University, Nishihiraki-cho, Takano, Sakyo-ku, Kyoto 606-8103, Japan

[‡]Institute for Molecular Science, Okazaki, Aichi 444-8585, Japan and School of Physical Sciences, The Graduate University for Advanced Studies, Okazaki, Aichi 444-8585, Japan

## References

The complete description of reference [67] is as follows:

Schmidt, M. W.; Baldridge, K. K.; Boatz, J. A.; Elbert, S. T.; Gordon, M. S.; Jensen, J. H.; Koseki, S.; Matsunaga, N.; Nguyen, K. A.; Su, S.; Windus, T. L.; Dupuis, M.; Montgomery, J. A. *J. Comput. Chem.*, **1993**, 14, 1347-1363.

**Analytical MP2 free energy gradient in the 3D-RISM**

Prior to applying the Z-vector method, the RISM-CPHF equation in the closed-shell case is derived in both of the conventional and the three-regions 3D-RISM calculations, as shown in Eq. (S1),

$$
\begin{aligned}
&\sum_{j}^{\mathrm{occ}}\sum_{b}^{\mathrm{vir}}\left[(\varepsilon_a-\varepsilon_i)\delta_{ab}\delta_{ij}+A_{aibj}+2Y_{aibj}\right]U^X_{bj}\\
&=-\left(h^X_{ai}+\frac{1}{2}\sum_{\lambda\sigma}^{\mathrm{AO}}P^{\mathrm{HF}}_{\lambda\sigma}G^X_{ai\lambda\sigma}\right)+\frac{1}{2}\sum_{jk}^{\mathrm{occ}}A_{aijk}S^X_{jk}+S^X_{ai}\varepsilon_i\\
&\quad-\sum_s\int d\mathbf{r}\left[X^X_{s,ai}(\mathbf{r})w(\mathbf{r})+X_{s,ai}(\mathbf{r})w^X(\mathbf{r})+\sum_\alpha\left\{Q^X_{\alpha,ai}V_{\alpha s}(\mathbf{r})+Q_{\alpha,ai}V^X_{\alpha s}(\mathbf{r})\right\}\right]\rho g_s(\mathbf{r})\\
&\quad-\sum_s\int d\mathbf{r}\left\{X_{s,ai}(\mathbf{r})w(\mathbf{r})+\sum_\alpha Q_{\alpha,ai}V_{\alpha s}(\mathbf{r})\right\}\rho g^X_s(\mathbf{r})+\sum_{jk}^{\mathrm{occ}}S^X_{jk}Y_{aijk},
\end{aligned}
\tag{S1}
$$

where $U^X_{pq}$ is the CPHF coefficient and $A_{\mu\nu pq}$ is the sum of $G_{\mu\nu pq}$ and $G_{\mu\nu qp}$; see Refs. [1] and [2] for the gas phase and the PCM calculations, respectively. $X_{s,\mu\nu}(\mathbf{r})$, $V_{\alpha s}(\mathbf{r})$, and $Y_{\mu\nu pq}$ in Eq. (S1) are defined by Eqs. (S2)-(S5),

$$
X_{s,\mu\nu}(\mathbf{r}) = -\langle\chi_\mu\,|\sum_{i\in\mathrm{electron}}\frac{q_s}{|\hat{\mathbf{r}}_i-\mathbf{r}|}\,|\,\chi_\nu\rangle-\sum_\alpha Q_{\alpha,\mu\nu}V_{\alpha s}(\mathbf{r}), \tag{S2}
$$

$$
V_{\alpha s}(\mathbf{r}) \equiv \frac{q_s}{|\mathbf{R}_\alpha-\mathbf{r}|}, \tag{S3}
$$

$$
Y_{\mu\nu pq} = \sum_s\int d\mathbf{r}\left\{X_{s,\mu\nu}(\mathbf{r})w(\mathbf{r})+\sum_\alpha Q_{\alpha,\mu\nu}V_{\alpha s}(\mathbf{r})\right\}Z_{s,pq}(\mathbf{r}), \tag{S4}
$$

$$
Z_{s,pq}(\mathbf{r}) \equiv \rho\sum_{\lambda\sigma}\left\{c_{\lambda p}c_{\sigma q}\left.\frac{\partial g_s}{\partial P_{\lambda\sigma}}\right|_{\mathbf{R}}(\mathbf{r})+c_{\lambda q}c_{\sigma p}\left.\frac{\partial g_s}{\partial P_{\lambda\sigma}}\right|_{\mathbf{R}}(\mathbf{r})\right\}, \tag{S5}
$$

where $c_{\mu p}$ is the MO coefficient at the RHF level.

Using the above CPHF coefficients $\{U^X_{ai}\}$, the first derivatives of the second order correlation energy $E^{(2)}$ with respect to nuclear coordinates $\mathbf{R}_\alpha$ are evaluated by Eq. (S6),

$$
\begin{aligned}
\frac{\partial E^{(2)}}{\partial \mathbf{R}_\alpha} &= \sum_{\mu\nu} h^X_{\mu\nu}\left\{2\sum_{ij} c_{\mu i}c_{\nu j}P^{(2)}_{ij} + 2\sum_{ab} c_{\mu a}c_{\nu b}P^{(2)}_{ab}\right\} \\
&+ \sum_{\mu\nu\lambda\sigma}(\mu\nu\,|\,\lambda\sigma)^X\left\{2\sum_{ijab} c_{\mu i}c_{\nu a}c_{\lambda j}c_{\sigma b}t^{ab}_{ij} + \left(\sum_{ij} c_{\mu i}c_{\nu j}P^{(2)}_{ij} + \sum_{ab} c_{\mu a}c_{\nu b}P^{(2)}_{ab}\right)P^{\mathrm{HF}}_{\lambda\sigma}\right\} \\
&+ \sum_{\mu\nu}\left\{2\sum_{ij} c_{\mu i}c_{\nu j}P^{(2)}_{ij} + 2\sum_{ab} c_{\mu a}c_{\nu b}P^{(2)}_{ab}\right\} \times \sum_s \int d\mathbf{r}\,\Big[ \\
&\quad \left\{X^X_{s,\mu\nu}(\mathbf{r})w(\mathbf{r}) + X_{s,\mu\nu}(\mathbf{r})w^X(\mathbf{r}) + \sum_\alpha\left(Q^X_{\alpha,ai}V_{\alpha s}(\mathbf{r}) + Q_{\alpha,ai}V^X_{\alpha s}(\mathbf{r})\right)\right\}\rho g_s(\mathbf{r}) + \\
&\quad \left\{X_{s,\mu\nu}(\mathbf{r})w(\mathbf{r}) + \sum_\alpha Q_{\alpha,ai}V_{\alpha s}(\mathbf{r})\right\}\rho g^X_s(\mathbf{r})\,\Big] \\
&+ \sum_{ab} S^X_{ab}\left\{-2\sum_{ijc} t^{bc}_{ij}(ia\,|\,jc) - (\varepsilon_a+\varepsilon_b)P^{(2)}_{ab}\right\} + \sum_{ia} S^X_{ai}\left\{-4\sum_{jkb} t^{ab}_{jk}(ji\,|\,kb)\right\} \\
&+ \sum_{ij} S^X_{ij}\Big[ -2\sum_{kab} t^{ab}_{jk}(ia\,|\,kb) - (\varepsilon_i+\varepsilon_j)P^{(2)}_{ij} - \\
&\quad \left\{\sum_{kl} P^{(2)}_{kl}\left(A_{klij}+2Y_{klij}\right) + \sum_{ab} P^{(2)}_{ab}\left(A_{abij}+2Y_{abij}\right)\right\}\Big] \\
&+ \sum_{ia} U^X_{ai}\Big[ -4\sum_{jkb} t^{ab}_{jk}(ji\,|\,kb) + 4\sum_{jbc} t^{bc}_{ij}(ab\,|\,jc) + \\
&\quad 2\left\{\sum_{jk} P^{(2)}_{jk}\left(A_{jkai}+2Y_{jkai}\right) + \sum_{bc} P^{(2)}_{bc}\left(A_{bcai}+2Y_{bcai}\right)\right\}\Big]. \qquad \text{(S6)}
\end{aligned}
$$

Here $P^{(2)}_{ij}$, $P^{(2)}_{ab}$, and $t^{ab}_{ij}$ are defined by

$$
\begin{aligned}
P^{(2)}_{ij} &= -\sum_k^{\mathrm{occ}}\sum_{ab}^{\mathrm{vir}} t^{ab}_{ij}(\varepsilon_i+\varepsilon_k-\varepsilon_a-\varepsilon_b)^{-1}(ia\,|\,kb), \qquad \text{(S7)} \\
P^{(2)}_{ab} &= +\sum_{ij}^{\mathrm{occ}}\sum_c^{\mathrm{vir}} t^{bc}_{ij}(\varepsilon_i+\varepsilon_j-\varepsilon_a-\varepsilon_c)^{-1}(ia\,|\,jc), \qquad \text{(S8)} \\
t^{ab}_{ij} &\equiv \frac{G_{ia\,jb}}{(\varepsilon_i+\varepsilon_j-\varepsilon_a-\varepsilon_b)}. \qquad \text{(S9)}
\end{aligned}
$$


[1]: Fletcher, G. D.; Rendell, A. P.; Sherwood, P. *Mol. Phys.* **1997**, 91, 431.

[2]: Cammi, R.; Mennucci, B.; Tomasi, J. *J. Phys. Chem.* **1999**, 103, 9100-9108.

**Z-vector method for the analytical MP2 free energy gradient in the 3D-RISM**

Applying the Z-vector method to Eqs. (S1) and (S6) in the same manner as Ref. [1], we can derive the new form of CPHF equation and simplify the first derivatives of $E^{(2)}$ in the 3D-RISM-MP2, as follows: The CPHF equation, $\sum_{ai} P^{(2)}_{ai} W_{aibj} = L_{bj}$, can be written by the matrices $\{L_{ai}\}$ and $W_{aibj}$ which are defined by Eqs. (S10) and (S11), respectively,

$$\begin{aligned} L_{ai} &\equiv \sum_{jkb} t^{ab}_{jk}(ji|kb) - \sum_{jbc} t^{bc}_{ij}(ab|jc) - \\ &\quad \frac{1}{2}\left\{ \sum_{jk} P^{(2)}_{jk}\left(A_{jkai} + 2Y_{jkai}\right) + \sum_{bc} P^{(2)}_{bc}\left(A_{bcai} + 2Y_{bcai}\right) \right\}, \qquad \text{(S10)} \\ W_{aibj} &\equiv \sum_{j}^{\text{occ}} \sum_{b}^{\text{vir}} \left[ (\varepsilon_a - \varepsilon_i)\delta_{ab}\delta_{ij} + A_{aibj} + 2Y_{aibj} \right]. \qquad \text{(S11)} \end{aligned}$$

Using this CPHF equation, we can reduce the computational cost to evaluate the last term of Eq. (S6), as shown in Eq. (S12),

$$-4\sum_{ai} U^X_{ai} L_{ai} = -4\sum_{aibj} U^X_{ai} W_{bjai} P^{(2)}_{bj} = -4\sum_{bj} P^{(2)}_{bj} B^X_{bj}, \qquad \text{(S12)}$$

where the matrix $\{B^X_{ai}\}$ is defined by Eq. (S13), and $\sum_{bj} W_{aibj} U^X_{bj} = B^X_{ai}$ was used in the second relation.

$$\begin{aligned} B^X_{ai} &\equiv -\left( h^X_{ai} + \frac{1}{2}\sum_{\lambda\sigma} P^{\text{HF}}_{\lambda\sigma} G^X_{ai\lambda\sigma} \right) + \frac{1}{2}\sum_{jk} A_{aijk} S^X_{jk} + S^X_{ai}\varepsilon_i \\ &\quad - \sum_s \int d\mathbf{r} \left[ X^X_{s,ai}(\mathbf{r}) w(\mathbf{r}) + X_{s,ai}(\mathbf{r}) w^X(\mathbf{r}) + \sum_\alpha \left\{ Q^X_{\alpha,ai} V_{\alpha s}(\mathbf{r}) + Q_{\alpha,ai} V^X_{\alpha s}(\mathbf{r}) \right\} \right] \rho g_s(\mathbf{r}) \\ &\quad - \sum_s \int d\mathbf{r} \left\{ X_{s,ai}(\mathbf{r}) w(\mathbf{r}) + \sum_\alpha Q_{\alpha,ai} V_{\alpha s}(\mathbf{r}) \right\} \rho g^X_s(\mathbf{r}) + \sum_{jk} S^X_{jk} Y_{aijk}. \qquad \text{(S13)} \end{aligned}$$

Summarizing the above equations, the CPHF equation is defined by Eq. (S14) and thereby the first derivatives of $E^{(2)}$ is evaluated by Eq. (S15),

$$
\begin{aligned}
&\sum_{j}^{\text{occ}}\sum_{b}^{\text{vir}}\left[(\varepsilon_a-\varepsilon_i)\delta_{ab}\delta_{ij}+A_{bjai}+2Y_{bjai}\right]P^{(2)}_{bj}\\
&\quad=\sum_{jk}^{\text{occ}}\sum_{b}^{\text{vir}}t^{ab}_{jk}(ji\,|\,kb)-\frac{1}{2}\sum_{jk}^{\text{occ}}P^{(2)}_{jk}\left[A_{jkai}+2Y_{jkai}\right]\\
&\quad-\sum_{j}^{\text{occ}}\sum_{bc}^{\text{vir}}t^{bc}_{ij}(ab\,|\,jc)-\frac{1}{2}\sum_{bc}^{\text{vir}}P^{(2)}_{bc}\left[A_{bcai}+2Y_{bcai}\right],
\end{aligned}
\tag{S14}
$$

$$
\begin{aligned}
\frac{\partial E^{(2)}}{\partial \mathbf{R}_\alpha} &= \sum_{\mu\nu}^{\text{AO}}h^X_{\mu\nu}P^{(2)}_{\mu\nu}+\sum_{\mu\nu}^{\text{AO}}S^X_{\mu\nu}W^{(2)}_{\mu\nu}+\sum_{\mu\nu\lambda\sigma}^{\text{AO}}(\mu\nu\,|\,\lambda\sigma)^X\Gamma^{(2)}_{\mu\nu\lambda\sigma}\\
&+\sum_{\mu\nu}P^{(2)}_{\mu\nu}\sum_s\int d\mathbf{r}\left\{X^X_{s,\mu\nu}(\mathbf{r})w(\mathbf{r})+X_{s,\mu\nu}(\mathbf{r})w^X(\mathbf{r})\right\}\rho g_s(\mathbf{r})\\
&+\sum_{\mu\nu}P^{(2)}_{\mu\nu}\sum_s\int d\mathbf{r}\sum_\alpha\left\{Q^X_{\alpha,\mu\nu}V_{\alpha s}(\mathbf{r})+Q_{\alpha,\mu\nu}V^X_{\alpha s}(\mathbf{r})\right\}\rho g_s(\mathbf{r})\\
&+\sum_{\mu\nu}P^{(2)}_{\mu\nu}\sum_s\int d\mathbf{r}\left\{X_{s,\mu\nu}(\mathbf{r})w(\mathbf{r})+\sum_\alpha Q_{\alpha,\mu\nu}V_{\alpha s}(\mathbf{r})\right\}\rho g^X_s(\mathbf{r}),
\end{aligned}
\tag{S15}
$$

where $P^{(2)}_{ai}$ is equal to $P^{(2)}_{ia}$ and $\Gamma^{(2)}_{\mu\nu\lambda\sigma}$ and $W_{\mu\nu}$ are defined by Eqs. (S16)-(S20), respectively,

$$
\Gamma^{(2)}_{\mu\nu\lambda\sigma} = 2\sum_{ijab}c_{\mu i}c_{\nu a}c_{\lambda j}c_{\sigma b}t^{ab}_{ij}+\frac{1}{2}\left(2P^{(2)}_{\mu\nu}P^{\text{HF}}_{\lambda\sigma}-P^{(2)}_{\mu\sigma}P^{\text{HF}}_{\lambda\nu}\right),
\tag{S16}
$$

$$
W^{(2)}_{\mu\nu} = 2\sum_{pq}c_{\mu p}c_{\nu q}W^{(2)}_{pq},
\tag{S17}
$$

$$
W^{(2)}_{ai} = W^{(2)}_{ia}\equiv-\sum_{jk}t^{ab}_{jk}(ji\,|\,kb)-\varepsilon_iP^{(2)}_{ai},
\tag{S18}
$$

$$
W^{(2)}_{ab} \equiv -\sum_{ijc}t^{bc}_{ij}(ia\,|\,jc)-\frac{1}{2}(\varepsilon_a+\varepsilon_b)P^{(2)}_{ab},
\tag{S19}
$$

$$
W^{(2)}_{ij} \equiv -\sum_{kab}t^{ab}_{jk}(ia\,|\,kb)-\frac{1}{2}(\varepsilon_i+\varepsilon_j)P^{(2)}_{ij}-\frac{1}{2}\sum_{pq}P^{(2)}_{pq}[A_{pqij}+2Y_{pqij}].
\tag{S20}
$$

[1]: Handy, N. C.; Schaefer III, H. F. *J. Chem. Phys.* **1984**, 81, 5031; Handy, N. C.; Amos, R. D.; Gaw, J. F.; Rice, J. E.; Simandiras, E. D. *Chem. Phys. Lett.* **1985**, 120, 151;

**Approximated MP2 free energy gradient in the three-regions 3D-RISM**

To determine $\{P_{ai}^{(2)}\}$ in Eq. (S14) and evaluate the first derivatives of $E^{(2)}$ in Eq. (S15), both of $Y_{\mu\nu pq}$ and $g_s^X(\mathbf{r})$ must be calculated for the 3D-RISM-MP2 free energy gradient; see Supporting Information pages S9-S10 for the details of the latter term. In the conventional 3D-RISM-MP2, where the pure point charge approximation is applied, $Y_{\mu\nu pq}$ can be evaluated at a moderate computational cost; the reason will be discussed below. In the three-regions 3D-RISM-MP2, however, the evaluation of $Y_{\mu\nu pq}$ needs very long CPU time and huge computational costs when $N_{\mathrm{AO}} \times N_{\mathrm{AO}}$ elements of $\{\partial g_s/\partial P_{\mu\nu}\}$ are accurately determined by solving the CP-RISM equation. To reduce the computational cost, we evaluate $Y_{\mu\nu pq}$ in the three-regions 3D-RISM-MP2 by assuming the pure point charge approximation.

When the pure point charge approximation is applied to the RISM-CPHF equation, $\{\partial g_s/\partial P_{\mu\nu}\}$ can be simply evaluated by Eq. (S21) like the 1D-RISM-MP2 in Ref. [1],

$$\left.\frac{\partial g_s}{\partial P_{\mu\nu}}\right|_{\mathbf{R}}(\mathbf{r}) = \sum_{\alpha} Q_{\alpha,\mu\nu} \left.\frac{\partial g_s}{\partial Q_\alpha}\right|_{\mathbf{R}}(\mathbf{r}). \tag{S21}$$

This indicates that only $N_{\mathrm{solute}}$ elements of $\{\partial g_s/\partial Q_\alpha\}$ must be determined by the CP-RISM equation and hence the CPU time is drastically reduced.

Next, we elucidate the CP-RISM equation under the pure point charge approximation. When the hyper-netted chain (HNC) closure [2] is used, $\{\partial g_s/\partial Q_\alpha\}$ can be evaluated by Eqs. (S22)-(S25),

$$\frac{\partial g_s}{\partial Q_\alpha}(\mathbf{r}) = \left(-\beta\frac{\partial u_s^s}{\partial Q_\alpha}(\mathbf{r}) + \frac{\partial \theta_s}{\partial Q_\alpha}(\mathbf{r}) + \frac{\partial \gamma_s}{\partial Q_\alpha}(\mathbf{r})\right) g_s(\mathbf{r}), \tag{S22}$$

$$\frac{\partial \widetilde{\theta}_s}{\partial Q_\alpha}(\mathbf{k}) = \sum_{s'} \frac{\partial \widetilde{c}_{s'}^s}{\partial Q_\alpha}(\mathbf{k})\widetilde{H}_{s's}(\mathbf{k}) - \frac{\partial \widetilde{c}_s^s}{\partial Q_\alpha}(\mathbf{k}), \tag{S23}$$

$$\frac{\partial c_s^s}{\partial Q_\alpha}(\mathbf{r}) = \left(-\beta\frac{\partial u_s^s}{\partial Q_\alpha} + \frac{\partial \theta_s}{\partial Q_\alpha} + \frac{\partial \gamma_s}{\partial Q_\alpha}\right) g_s(\mathbf{r}) - \left(\frac{\partial \theta_s}{\partial Q_\alpha} + \frac{\partial \gamma_s}{\partial Q_\alpha}\right), \tag{S24}$$

$$g_s(\mathbf{r}) \equiv h_s(\mathbf{r}) + 1 = \exp[c_s^s(\mathbf{r}) + \theta_s(\mathbf{r}) + \gamma_s(\mathbf{r})], \tag{S25}$$

where the tilde denotes the quantity in reciprocal space, $h_s$ and $c_s^s$ are the total and the short-range direct correlation functions, respectively, which are determined by the 3D-RISM equation as well as $\theta_s$. $\gamma_s$, $\partial u_s^s/\partial Q_\alpha$, and $\partial\gamma_s/\partial Q_\alpha$ are defined by

$$\widetilde{\gamma}_s(\mathbf{k}) = -\beta\sum_{s'}\widetilde{u}_{s'}^l(\mathbf{k})\tilde{H}_{s's}(\mathbf{k}), \tag{S26}$$

$$\frac{\partial u_s^s}{\partial Q_\alpha}(\mathbf{r}) = V_{\alpha s}(\mathbf{r}) - \frac{\partial u_s^l}{\partial Q_\alpha}(\mathbf{r}), \tag{S27}$$

$$\frac{\partial\widetilde{\gamma}_s}{\partial Q_\alpha}(\mathbf{k}) = -\beta\sum_{s'}\frac{\partial\widetilde{u}_{s'}^l}{\partial Q_\alpha}(\mathbf{k})\widetilde{H}_{s's}(\mathbf{k}), \tag{S28}$$

where the pure point charge approximation is used in Eq. (S27) and $u_s^l$ is the long-range electrostatic (ES) interaction energy between the solvent site $s$ and the solute molecule.

When the ESP charges are converged in the SCF manner, the pure point charge approximation works well in the evaluation of $\partial g_s/\partial P_{\mu\nu}$, because the long-range term of $\partial u_s/\partial P_{\mu\nu}$ ($\propto 1/r$) can mainly contribute to $\partial g_s/\partial P_{\mu\nu}$; remember that the three-regions 3D-RISM-SCF calculation provides the good convergence of the ESP charges on the solute sites. These calculated ESP charges quantitatively reproduce the ESP around the solute molecule, solvation free energy, and the profile of the free energy directly calculated with the wave-functions when the ESP charges are successfully converged.

[1]: Mori, T.; Kato, S. *Chem. Phys. Lett.* **2007**, 437, 159-163.

[2]: Singer, S. J.; Chandler, D. *Mol. Phys.* **1985**, 55, 621-625; Chandler, D.; Singh, Y.; Richardson, D. M. *J. Chem. Phys.* **1984**, 81, 1975-1982.

**Z-vector method for the CP-RISM equation**

Prior to applying the Z-vector method to the CP-RISM equation, we elucidate the the evaluation of $\{g_s^X(\mathbf{r})\}$ in the conventional and the three-regions 3D-RISM-MP2 calculations. In the similar manner to the CP-RISM equation for $\{\partial g_s/\partial Q_\alpha\}$, $\{g_s^X(\mathbf{r})\}$ can be evaluated by solving Eqs. (S29)-(S31),

$$g_s^X(\mathbf{r}) = \left(-\beta \left.\frac{\partial u_s^s}{\partial \mathbf{R}_\alpha}\right|_{\mathbf{P}}(\mathbf{r}) + \left.\frac{\partial \theta_s}{\partial \mathbf{R}_\alpha}\right|_{\mathbf{P}}(\mathbf{r}) + \left.\frac{\partial \gamma_s}{\partial \mathbf{R}_\alpha}\right|_{\mathbf{P}}(\mathbf{r})\right) g_s(\mathbf{r}), \tag{S29}$$

$$\frac{\partial \widetilde{\theta}_s}{\partial \mathbf{R}_\alpha}(\mathbf{k}) = \sum_{s'} \frac{\partial \widetilde{c}_{s'}^s}{\partial \mathbf{R}_\alpha}(\mathbf{k})\widetilde{H}_{s's}(\mathbf{k}) - \frac{\partial \widetilde{c}_s^s}{\partial \mathbf{R}_\alpha}(\mathbf{k}), \tag{S30}$$

$$\frac{\partial c_s^s}{\partial \mathbf{R}_\alpha}(\mathbf{r}) = \left(-\beta \frac{\partial u_s^s}{\partial \mathbf{R}_\alpha} + \frac{\partial \theta_s}{\partial \mathbf{R}_\alpha} + \frac{\partial \gamma_s}{\partial \mathbf{R}_\alpha}\right) g_s(\mathbf{r}) - \left(\frac{\partial \theta_s}{\partial \mathbf{R}_\alpha} + \frac{\partial \gamma_s}{\partial \mathbf{R}_\alpha}\right), \tag{S31}$$

where the HNC closure is used in Eq. (S31) and $u_s^s$ is defined in both of the conventional and the three-regions 3D-RISM-SCF calculations by Eqs. (S32) and (S33),

$$u_s^s(\mathbf{r}) = \sum_{\mu\nu} P_{\mu\nu}^{\mathrm{HF}} X_{s,\mu\nu}(\mathbf{r}) w(\mathbf{r}) + \sum_\alpha Q_\alpha V_{\alpha s}(\mathbf{r}) + u_s^{\mathrm{LJ}}(\mathbf{r}) - u_s^l(\mathbf{r}), \tag{S32}$$

$$u_s^l(\mathbf{r}) = q_s \sum_\alpha \frac{(Q_\alpha + Z_\alpha)\,\mathrm{erf}(\lambda \mid \mathbf{r} - \mathbf{R}_\alpha \mid)}{\mid \mathbf{r} - \mathbf{R}_\alpha \mid}. \tag{S33}$$

Although the above CP-RISM equation provides $3 \times N_{\mathrm{solute}}$ elements of $\{\partial g_s/\partial \mathbf{R}_\alpha\}$ straightforwardly, we wish to reduce the computational cost of the CP-RISM calculations by using the Z-vector method. Strictly speaking, the evaluation of the last term of Eq. (S15) does not explicitly use all the elements of $\{\partial g_s/\partial \mathbf{R}_\alpha\}$, as discussed below. To apply the Z-vector method, the last term in Eq. (S15) is transformed, as shown in Eq. (S34),

$$\sum_{\mu\nu} P_{\mu\nu}^{(2)} \sum_s \int d\mathbf{r} \left\{ X_{s,\mu\nu}(\mathbf{r}) w(\mathbf{r}) + \sum_\alpha Q_{\alpha,\mu\nu} V_{\alpha s}(\mathbf{r}) \right\} \rho g_s^X(\mathbf{r}) = E_1^{(2)X} + E_2^{(2)X}, \tag{S34}$$

where the first and the second terms are defined by Eqs. (S35) and (S36),

$$E_1^{(2)X} \equiv \sum_{\mu\nu} P_{\mu\nu}^{(2)} \sum_s \int d\mathbf{r} \left\{ X_{s,\mu\nu} w + \sum_\alpha Q_{\alpha,\mu\nu} V_{\alpha s} \right\} \rho \frac{\partial \theta_s}{\partial \mathbf{R}_\alpha} g_s, \tag{S35}$$

$$E_2^{(2)X} \equiv \sum_{\mu\nu} P_{\mu\nu}^{(2)} \sum_s \int d\mathbf{r} \left\{ X_{s,\mu\nu} w + \sum_\alpha Q_{\alpha,\mu\nu} V_{\alpha s} \right\} \rho \left( -\beta \frac{\partial u_s^s}{\partial \mathbf{R}_\alpha} + \frac{\partial \gamma_s}{\partial \mathbf{R}_\alpha} \right) g_s. \tag{S36}$$

The calculation of $E_1^{(2)X}$ requires the CP-RISM equation, while that of $E_2^{(2)X}$ only uses the correlation functions which are determined by the 3D-RISM equation. Applying the Z-vector method, $E_1^{(2)X}$ is further transformed to the convenient form of Eq. (S37),

$$\begin{aligned} E_1^{(2)X} &= \sum_{\mu\nu} P_{\mu\nu}^{(2)} \sum_s \int d\mathbf{r} \left\{ X_{s,\mu\nu} w + \sum_\alpha Q_{\alpha,\mu\nu} V_{\alpha s} \right\} \rho g_s \left( \text{I.F.T.} \left[ \sum_{s'} \frac{\partial \widetilde{c}_{s'}^s}{\partial \mathbf{R}_\alpha} \widetilde{H}_{s's} \right] - \frac{\partial c_s^s}{\partial \mathbf{R}_\alpha} \right), \\ &= \rho \sum_s \int d\mathbf{r} \left( \text{I.F.T.} \left[ \sum_{s'} \widetilde{\Psi}_{s'}(\mathbf{k}) \widetilde{H}_{s's}(\mathbf{k}) \right] - \Psi_s(\mathbf{r}) \right) I_s^X(\mathbf{r}), \end{aligned} \tag{S37}$$

where the F.T. and I.F.T. denote Fourier and inverse-Fourier transformations, respectively, and $I_s^X$ is defined by Eq. (S38),

$$I_s^X(\mathbf{r}) = (g_s(\mathbf{r}) - 1)\gamma_s^X(\mathbf{r}) + g_s(\mathbf{r})(-\beta u_s^{sX}(\mathbf{r})). \tag{S38}$$

$\Psi_s$ in Eq. (S37) is determined by solving the new CP-RISM equation in Eqs. (S39)-(S41),

$$\widetilde{\Theta}_s(\mathbf{k}) = \sum_{s'} \widetilde{\Psi}_{s'}(\mathbf{k}) \widetilde{H}_{s's}(\mathbf{k}) - \Psi_s(\mathbf{r}), \tag{S39}$$

$$\Psi_s(\mathbf{r}) = (g_s(\mathbf{r}) - 1)\Theta_s(\mathbf{r}) + \psi_s^{(2)}(\mathbf{r}), \tag{S40}$$

$$\psi_s^{(2)}(\mathbf{r}) \equiv \sum_{\mu\nu} P_{\mu\nu}^{(2)} \left\{ X_{s,\mu\nu}(\mathbf{r}) w(\mathbf{r}) + \sum_\alpha Q_{\alpha,\mu\nu} V_{\alpha s}(\mathbf{r}) \right\} g_s(\mathbf{r}), \tag{S41}$$

This new CP-RISM equation is calculated only once to evaluate $E_1^{(2)X}$, indicating that the CPU time can be reduced drastically by the Z-vector method. In the charged system, it will be practically better to partition $\psi_s^{(2)}$ into the short-range and the long-range functions in the above equations, which is straightforward and thus not shown here.

In this Supporting Information, the free energy gradient was discussed at the restricted MP2 level but those at the restricted open shell and unrestricted MP2 levels can be also straightforwardly derived by the same procedure.

**Detailed comparison of $E_{\mathrm{bind}}^{\mathrm{MP2}}$ and $\Delta\Delta\mu^{\mathrm{MP2}}$ between the H-ahead and O-ahead hydrations**

Table 3 lists the binding free energy $A_{\mathrm{bind}}^{\mathrm{MP2}}$, the solute binding energy $E_{\mathrm{bind}}^{\mathrm{MP2}}$, and the solvation free energy $\Delta\mu_{\mathrm{rism}}^{\mathrm{MP2}}$. As one example, let's consider the difference in stability ($\Delta\Delta A_{\mathrm{bind}}^{\mathrm{MP2}}(\mathrm{H}-\mathrm{O})$) between the H-ahead and O-ahead hydrations of the glycine complex; the negative value represents that the H-ahead mode is more stable than the O-ahead one. $\Delta A_{\mathrm{bind}}^{\mathrm{MP2}}(\mathrm{H}-\mathrm{O})$ indicates that the H-ahead hydration is more stable than the O-ahead one by 2.5 kcal/mol in **1a** but only 0.1 kcal/mol in **2a**. $\Delta\Delta\mu^{\mathrm{MP2}}$ less stabilizes the H-ahead hydration than the O-ahead one by 1.2 kcal/mol in **1a** and 1.5 kcal/mol in **2a**; in other words, this term is not very different between **1a** and **2a**. However, $E_{\mathrm{int}}^{\mathrm{MP2}}$ differs between them because it more stabilizes the H-ahead hydration than the O-ahead one by 3.4 kcal/mol in **1a** and 1.2 kcal/mol in **2a**. These results indicate that the difference in $E_{\mathrm{int}}^{\mathrm{MP2}}$ between the H-ahead and O-ahead hydrations is responsible for the difference in $\Delta A_{\mathrm{bind}}^{\mathrm{MP2}}(\mathrm{H}-\mathrm{O})$ between **1a** and **2a**.

In the charged systems **1b**, **2b**, **1c**, and **2c**, the differences in $\Delta\Delta\mu_{\mathrm{rism}}^{\mathrm{MP2}}$ between the H-ahead and O-ahead hydrations are similar between the Pt and Pd complexes but influence the relative stabilities of the H-ahead and O-ahead modes like in **1a** and **2a**. If we compare the relative stabilities of H-ahead and O-ahead hydrations of **1b** between gas and aqueous phases, $E_{\mathrm{bind}}^{\mathrm{MP2}}$ in gas phase was much more positive in the H-ahead hydration than in the O-ahead one by 14.1 kcal/mol. In contrast, the difference in $A_{\mathrm{bind}}^{\mathrm{MP2}}$ between these two hydrations indicates that the H-ahead hydration is slightly more stable than the O-ahead one by 0.3 kcal/mol in aqueous phase. The large increase in the stability of the H-ahead hydration arises from the more negative $\Delta\Delta\mu_{\mathrm{rism}}^{\mathrm{MP2}}$ in the the H-ahead hydration than in the O-ahead one by 18.1 kcal/mol which compensates the more positive $E_{\mathrm{bind}}^{\mathrm{MP2}}$ in the H-ahead hydration than in the O-ahead one by 17.8 kcal/mol. In all other cases, $\Delta\Delta\mu_{\mathrm{rism}}^{\mathrm{MP2}}$ plays an important role in determining $A_{\mathrm{bind}}^{\mathrm{MP2}}$. It is also noted that in all cases, $\Delta\Delta\mu_{\mathrm{rism}}^{\mathrm{MP2}}$ decreases the difference in the relative stability between the two hydration modes.

Table S1: Stable structures determined by the full geometry optimizations.[a]

| | Pt complex | | | | | | | |
|---|---|---|---|---|---|---|---|---|
| | **1a**, $PtCl_2(NH_3)$(glycine) | | | | **1b**, $[Pt(NH_3)_4]^{2+}$ | | **1c**, $[Pt(CN)_4]^{2-}$ | |
| Geom.[b] | H-I | H-II | O-I | O-II | H-I | O-I | H-I | O-I |
| Existence[c] | yes (no[d]) | yes (no) | no (no) | yes (yes) | yes (no) | yes (yes) | no (no) | no (no) |
| $r$(Pt-$L^1$)[e] | 2.279 (-) | 2.282 (-) | - (-) | 2.283 (2.294) | 2.021 (-) | 2.023 (2.042) | - (-) | - (-) |
| $r$(Pt-$L^2$) | 2.276 (-) | 2.275 (-) | - (-) | 2.283 (2.294) | 2.023 (-) | 2.023 (2.042) | - (-) | - (-) |
| $r$(Pt-$L^3$) | 2.017 (-) | 2.019 (-) | - (-) | 2.018 (2.019) | 2.023 (-) | 2.023 (2.043) | - (-) | - (-) |
| $r$(Pt-$L^4$) | 2.017 (-) | 2.019 (-) | - (-) | 2.017 (2.003) | 2.021 (-) | 2.023 (2.043) | - (-) | - (-) |
| $r$(O-$H^1$) | 0.978 (-) | 0.978 (-) | - (-) | 0.970 (0.966) | 0.972 (-) | 0.971 (0.970) | - (-) | - (-) |
| $r$(O-$H^2$) | 0.971 (-) | 0.970 (-) | - (-) | 0.970 (0.966) | 0.970 (-) | 0.971 (0.970) | - (-) | - (-) |
| $r$(Pt-$H^1$) | 2.27 (-) | 2.25 (-) | - (-) | 3.85 (3.96) | 2.45 (-) | 3.99 (3.81) | - (-) | - (-) |
| $r$(Pt-O) | 3.25 (-) | 3.23 (-) | - (-) | 3.33 (3.31) | 3.38 (-) | 3.32 (3.12) | - (-) | - (-) |
| | Pd complex | | | | | | | |
| | **2a**, $PdCl_2(NH_3)$(glycine) | | | | **2b**, $[Pd(NH_3)_4]^{2+}$ | | **2c**, $[Pd(CN)_4]^{2-}$ | |
| Geom.[b] | H-I | H-II | O-I | O-II | H-I | O-I | H-I | O-I |
| Existence[c] | yes (no[d]) | yes (no) | yes (no) | yes (yes) | no (no) | yes (yes) | no (no) | no (no) |
| $r$(Pd-$L^1$)[e] | 2.278 (-) | 2.278 (-) | 2.294 (-) | 2.291 (2.294) | - (-) | 2.028 (2.053) | - (-) | - (-) |
| $r$(Pd-$L^2$) | 2.276 (-) | 2.277 (-) | 2.294 (-) | 2.292 (2.294) | - (-) | 2.028 (2.054) | - (-) | - (-) |
| $r$(Pd-$L^3$) | 2.015 (-) | 2.017 (-) | 2.013 (-) | 2.015 (2.024) | - (-) | 2.028 (2.054) | - (-) | - (-) |
| $r$(Pd-$L^4$) | 2.019 (-) | 2.020 (-) | 2.022 (-) | 2.020 (2.010) | - (-) | 2.027 (2.054) | - (-) | - (-) |
| $r$(O-$H^1$) | 0.970 (-) | 0.971 (-) | 0.970 (-) | 0.970 (0.966) | - (-) | 0.971 (0.970) | - (-) | - (-) |
| $r$(O-$H^2$) | 0.971 (-) | 0.970 (-) | 0.969 (-) | 0.970 (0.965) | - (-) | 0.970 (0.970) | - (-) | - (-) |
| $r$(Pd-$H^1$) | 2.36 (-) | 2.40 (-) | 3.33 (-) | 3.65 (3.66) | - (-) | 3.64 (3.60) | (-) | (-) |
| $r$(Pd-O) | 3.33 (-) | 3.36 (-) | 2.97 (-) | 3.06 (3.00) | - (-) | 2.98 (2.91) | - (-) | - (-) |

[a]Calculated by three-regions 3D-RISM-MP2. Unit is in Å. [b,c]See caption of Table 1 in main text for notations. [d]In parentheses are gas phase optimization results. [e]($L^1$, $L^2$, $L^3$, $L^4$) represents (Cl, Cl, $N_{am}$, $N_{gly}$) in glycine complex, ($N_{am}$, $N_{am}$, $N_{am}$, $N_{am}$) in tetra-ammine complex, and ($C_{cy}$, $C_{cy}$, $C_{cy}$, $C_{cy}$) in tetra-cyano complex, where $N_{am}$, $N_{gly}$, and $C_{cy}$ represents the N atom on $NH_3$ ligand, the N atom on glycine ligand, and C atom on cyanide ligand, respectively.

Table S2: Stable structures determined by the partial geometry optimizations.[a]

| | Pt complex | | | | | | | |
|---|---|---|---|---|---|---|---|---|
| | **1a**, $PtCl_2(NH_3)$(glycine) | | | | **1b**, $[Pt(NH_3)_4]^{2+}$ | | **1c**, $[Pt(CN)_4]^{2-}$ | |
| Geom.[b] | H-I | H-II | O-I | O-II | H-I | O-I | H-I | O-I |
| Existence[c] | yes (yes[d]) | yes (yes) | yes (yes) | yes (yes) | yes (yes) | yes (yes) | yes (yes) | no[f] (no) |
| $r$(Pt-L$^1$)[e] | 2.280 (2.284) | 2.281 (2.288) | 2.285 (2.295) | 2.286 (2.294) | 2.022 (2.046) | 2.024 (2.041) | 1.954 (1.972) | 1.952 (-) |
| $r$(Pt-L$^2$) | 2.276 (2.291) | 2.277 (2.287) | 2.285 (2.295) | 2.286 (2.294) | 2.023 (2.045) | 2.023 (2.042) | 1.957 (1.974) | 1.956 (-) |
| $r$(Pt-L$^3$) | 2.016 (2.019) | 2.018 (2.018) | 2.015 (2.013) | 2.021 (2.016) | 2.022 (2.045) | 2.023 (2.043) | 1.954 (1.974) | 1.952 (-) |
| $r$(Pt-L$^4$) | 2.017 (2.008) | 2.021 (2.015) | 2.020 (2.009) | 2.011 (2.010) | 2.021 (2.045) | 2.023 (2.043) | 1.955 (1.973) | 1.952 (-) |
| $r$(O-H$^1$) | 0.976 (0.974) | 0.977 (0.976) | 0.969 (0.966) | 0.970 (0.966) | 0.971 (0.963) | 0.971 (0.969) | 0.978 (0.981) | 0.969 (-) |
| $r$(O-H$^2$) | 0.970 (0.966) | 0.971 (0.966) | 0.969 (0.966) | 0.970 (0.966) | 0.970 (0.965) | 0.971 (0.969) | 0.970 (0.966) | 0.969 (-) |
| $r$(Pt-H$^1$) | 2.29 (2.31) | 2.31 (2.29) | 3.81 (3.67) | 3.89 (4.03) | 2.48 (2.47) | 3.96 (3.78) | 2.26 (2.39) | 3.74 (-) |
| $r$(Pt-O) | 3.27 (3.29) | 3.29 (3.25) | 3.39 (3.07) | 3.37 (3.37) | 3.45 (3.43) | 3.36 (3.10) | 3.24 (3.37) | 3.39 (-) |
| | Pd complex | | | | | | | |
| | **2a**, $PdCl_2(NH_3)$(glycine) | | | | **2b**, $[Pd(NH_3)_4]^{2+}$ | | **2c**, $[Pd(CN)_4]^{2-}$ | |
| Geom.[b] | H-I | H-II | O-I | O-II | H-I | O-I | H-I | O-I |
| Existence[c] | yes (yes[d]) | yes (yes) | yes (yes) | yes (yes) | yes (yes) | yes (yes) | yes (yes) | no[f] (no) |
| $r$(Pd-L$^1$)[e] | 2.277 (2.278) | 2.279 (2.280) | 2.299 (2.299) | 2.296 (2.295) | 2.024 (2.054) | 2.025 (2.052) | 1.955 (1.977) | 1.955 (-) |
| $r$(Pd-L$^2$) | 2.276 (2.285) | 2.274 (2.284) | 2.299 (2.299) | 2.296 (2.295) | 2.024 (2.053) | 2.030 (2.053) | 1.956 (1.978) | 1.956 (-) |
| $r$(Pd-L$^3$) | 2.012 (2.026) | 2.015 (2.024) | 2.023 (2.017) | 2.015 (2.023) | 2.024 (2.052) | 2.030 (2.055) | 1.952 (1.977) | 1.953 (-) |
| $r$(Pd-L$^4$) | 2.023 (2.011) | 2.025 (2.021) | 2.007 (2.023) | 2.026 (2.022) | 2.022 (2.053) | 2.024 (2.054) | 1.956 (1.977) | 1.952 (-) |
| $r$(O-H$^1$) | 0.970 (0.969) | 0.970 (0.969) | 0.970 (0.966) | 0.970 (0.966) | 0.966 (0.961) | 0.971 (0.969) | 0.972 (0.976) | 0.969 (-) |
| $r$(O-H$^2$) | 0.970 (0.965) | 0.971 (0.965) | 0.970 (0.966) | 0.970 (0.966) | 0.970 (0.966) | 0.971 (0.969) | 0.971 (0.966) | 0.969 (-) |
| $r$(Pd-H$^1$) | 2.38 (2.37) | 2.39 (2.41) | 3.47 (3.46) | 3.70 (3.71) | 2.55 (2.50) | 3.67 (3.62) | 2.30 (2.45) | 3.38 (-) |
| $r$(Pd-O) | 3.35 (3.34) | 3.36 (3.38) | 2.99 (2.83) | 3.10 (3.05) | 3.51 (3.46) | 2.98 (2.93) | 3.27 (3.42) | 2.99 (-) |

[a]Calculated by three-regions 3D-RISM-MP2. Unit is in Å. [b,c]See caption of Table 2 in main text for notations. [d]In parentheses are gas phase optimization results. [e]See caption of Table S1 for notation. [f]Because the partial geometry optimization provided the unexpected result (neither O-ahead nor H-ahead mode), model geometries of **1c** and **2c** were determined by adding one more constraint that $r$(**M**-O) was fixed to that of **1a-O-I** and **2a-O-I**, respectively.

Table S3: Free energy and its components of the complex-water system.[a]

| | Pt complex | | | | | | | |
|---|---|---|---|---|---|---|---|---|
| | **1a**, $PtCl_2(NH_3)$(glycine) | | | | **1b**, $[Pt(NH_3)_4]^{2+}$ | | **1c**, $[Pt(CN)_4]^{2-}$ | |
| Geom. | H-I | H-II | O-I | O-II | H-I | O-I | H-I | O-I |
| $A_{\mathrm{bind}}^{\mathrm{MP2}}$ | -1.1 (-3.8[b]) | -1.0 (-4.6) | 1.4 (-0.7) | 0.7 (0.1) | 0.3 (2.7) | 0.6 (-11.3) | -1.0 (-8.4) | 0.8 (2.7) |
| components of $A_{\mathrm{bind}}^{\mathrm{MP2}}$ | | | | | | | | |
| $\Delta\Delta\mu_{\mathrm{rism}}^{\mathrm{MP2}}$ | 3.6 | 4.7 | 2.4 | 0.7 | -4.7 | 13.4 | 8.3 | -2.3 |
| $E_{\mathrm{bind}}^{\mathrm{MP2}}$ | -4.7 | -5.7 | -1.0 | 0.0 | 5.0 | -12.8 | -9.3 | 3.1 |
| components of $E_{\mathrm{bind}}^{\mathrm{MP2}}$ | | | | | | | | |
| $E_{\mathrm{int}}^{\mathrm{MP2}}$ | -4.0 | -4.8 | -0.6 | 0.3 | 3.0 | -11.2 | -8.2 | 3.2 |
| $\Delta E_{\mathrm{reorg}}^{\mathrm{MONOs,MP2}}$ | -0.8 | -1.2 | -0.5 | -0.3 | 1.9 | -1.6 | -1.3 | -0.1 |
| $\Delta E_{\mathrm{gas}}^{\mathrm{MONOs,MP2}}$ | 0.1 | 0.3 | 0.1 | 0.0 | 0.1 | 0.0 | 0.2 | 0.0 |
| | Pd complex | | | | | | | |
| | **2a**, $PdCl_2(NH_3)$(glycine) | | | | **2b**, $[Pd(NH_3)_4]^{2+}$ | | **2c**, $[Pd(CN)_4]^{2-}$ | |
| Geom. | H-I | H-II | O-I | O-II | H-I | O-I | H-I | O-I |
| $A_{\mathrm{bind}}^{\mathrm{MP2}}$ | 0.8 (-2.4[b]) | 1.2 (-3.0) | 0.9 (-1.6) | 0.3 (-0.8) | 2.1 (3.8) | 0.4 (-12.8) | 0.0 (-9.4) | 0.7 (3.2) |
| components of $A_{\mathrm{bind}}^{\mathrm{MP2}}$ | | | | | | | | |
| $\Delta\Delta\mu_{\mathrm{rism}}^{\mathrm{MP2}}$ | 4.6 | 6.0 | 3.1 | 1.3 | -3.6 | 14.9 | 8.5 | -2.8 |
| $E_{\mathrm{bind}}^{\mathrm{MP2}}$ | -3.8 | -4.8 | -2.2 | -1.0 | 5.7 | -14.5 | -8.5 | 3.5 |
| components of $E_{\mathrm{bind}}^{\mathrm{MP2}}$ | | | | | | | | |
| $E_{\mathrm{int}}^{\mathrm{MP2}}$ | -2.6 | -3.2 | -1.4 | -0.6 | 3.9 | -12.5 | -7.2 | 3.9 |
| $\Delta E_{\mathrm{reorg}}^{\mathrm{MONOs,MP2}}$ | -1.2 | -1.7 | -1.0 | -0.8 | 1.7 | -2.0 | -1.5 | -0.4 |
| $\Delta E_{\mathrm{gas}}^{\mathrm{MONOs,MP2}}$ | 0.0 | 0.1 | 0.2 | 0.4 | 0.1 | 0.0 | 0.2 | 0.0 |

[a]Calculated at the model geometry with three-regions 3D-RISM-MP2. Unit is in kcal/mol. [b]In parentheses are the binding energy in gas phase, $E_{\mathrm{bind}}^{\mathrm{MP2}}$.

Table S4: NBO charges on the complex-water system in the absence of the bulk solvation effect.[a]

| | Pt complex | | | | | | | |
|---|---|---|---|---|---|---|---|---|
| | **1a**, $PtCl_2(NH_3)$(glycine) | | | | **1b**, $[Pt(NH_3)_4]^{2+}$ | | **1c**, $[Pt(CN)_4]^{2-}$ | |
| Geom. | H-I | H-II | O-I | O-II | H-I | O-I | H-I | O-I |
| $q$(Pt) | 0.545 (-0.025[b]) | 0.547 (-0.024) | 0.590 (+0.018) | 0.591 (+0.019) | 0.723 (-0.019) | 0.759 (+0.018) | 0.393 (-0.020) | 0.422 (+0.008) |
| $q$(**W**) | -0.024 | -0.022 | 0.001 | 0.003 | -0.005 | 0.002 | -0.024 | 0.005 |
| $q$(**4L**) | -0.521 (+0.049) | -0.525 (+0.046) | -0.591 (-0.019) | -0.594 (-0.022) | 1.282 (+0.024) | 1.239 (-0.020) | -2.369 (+0.044) | -2.427 (-0.013) |
| components of **4L** | | | | | | | | |
| $q(L^1)$[c] | -0.550 (+0.020) | -0.551 (+0.020) | -0.577 (-0.006) | -0.577 (-0.007) | 0.321 (+0.006) | 0.309 (-0.006) | -0.587 (+0.015) | -0.606 (-0.004) |
| $q(L^2)$ | -0.560 (+0.010) | -0.561 (+0.009) | -0.577 (-0.007) | -0.577 (-0.007) | 0.321 (+0.007) | 0.310 (-0.005) | -0.599 (+0.005) | -0.609 (-0.004) |
| $q(L^3)$ | 0.296 (+0.010) | 0.295 (+0.009) | 0.286 (+0.001) | 0.283 (0.000) | 0.323 (+0.009) | 0.311 (-0.004) | -0.588 (+0.014) | -0.601 (+0.003) |
| $q(L^4)$ | 0.293 (+0.009) | 0.292 (+0.008) | 0.277 (-0.007) | 0.277 (-0.008) | 0.317 (+0.002) | 0.309 (-0.005) | -0.595 (+0.010) | -0.611 (-0.008) |
| | Pd complex | | | | | | | |
| | **2a**, $PdCl_2(NH_3)$(glycine) | | | | **2b**, $[Pd(NH_3)_4]^{2+}$ | | **2c**, $[Pd(CN)_4]^{2-}$ | |
| Geom. | H-I | H-II | O-I | O-II | H-I | O-I | H-I | O-I |
| $q$(Pd) | 0.575 (-0.037[b]) | 0.576 (-0.037) | 0.649 (+0.030) | 0.646 (+0.027) | 0.738 (-0.023) | 0.791 (+0.029) | 0.311 (-0.030) | 0.356 (+0.015) |
| $q$(**W**) | -0.008 | -0.007 | 0.004 | 0.004 | 0.001 | 0.004 | -0.007 | 0.009 |
| $q$(**4L**) | -0.567 (+0.045) | -0.569 (+0.044) | -0.653 (-0.034) | -0.650 (-0.031) | 1.261 (+0.022) | 1.205 (-0.033) | -2.304 (+0.037) | -2.365 (-0.024) |
| components of **4L** | | | | | | | | |
| $q(L^1)$[c] | -0.572 (+0.021) | -0.573 (+0.020) | -0.608 (-0.012) | -0.605 (-0.009) | 0.315 (+0.006) | 0.303 (-0.008) | -0.573 (+0.014) | -0.593 (-0.006) |
| $q(L^2)$ | -0.584 (+0.008) | -0.581 (+0.008) | -0.608 (-0.012) | -0.605 (-0.009) | 0.316 (+0.006) | 0.299 (-0.009) | -0.580 (+0.004) | -0.592 (-0.007) |
| $q(L^3)$ | 0.295 (+0.008) | 0.292 (+0.007) | 0.281 (+0.001) | 0.285 (-0.002) | 0.318 (+0.009) | 0.300 (-0.008) | -0.573 (+0.012) | -0.583 (+0.001) |
| $q(L^4)$ | 0.294 (+0.008) | 0.293 (+0.009) | 0.282 (-0.011) | 0.275 (-0.011) | 0.312 (+0.001) | 0.303 (-0.008) | -0.578 (+0.007) | -0.597 (-0.012) |

[a]Calculated at the model geometry with three-regions 3D-RISM-MP2. Unit is in *e*. [b]In parentheses are the change in NBO charge induced by **W** under the consideration of solvation around the super molecule, *i.e.* complex+**W**. [c]($L^1$, $L^2$, $L^3$, $L^4$) represents (Cl, Cl, Am, Gly) in glycine complex, (Am, Am, Am, Am) in tetra-ammine complex, and (Cy, Cy, Cy, Cy) in tetra-cyano complex, where Am, Gly, and Cy represent the $NH_3$, glycine, and cyanide ligands, respectively.

Table S5: NBO populations of valence orbitals on the metal center of the complex-water system in aqueous phase.[a]

| | Pt complex | | | | | | | |
|---|---|---|---|---|---|---|---|---|
| | **1a**, $PtCl_2(NH_3)$(glycine) | | | | **1b**, $[Pt(NH_3)_4]^{2+}$ | | **1c**, $[Pt(CN)_4]^{2-}$ | |
| Geom. | H-I | H-II | O-I | O-II | H-I | O-I | H-I | O-I |
| Pop.(6s) | 0.659 (0.640) | 0.660 (0.641) | 0.627 (0.644) | 0.628 (0.645) | 0.658 (0.645) | 0.637 (0.654) | 0.755 (0.747) | 0.738 (0.747) |
| Pop.($6p_z$) | 0.020 (0.017) | 0.020 (0.017) | 0.018 (0.017) | 0.018 (0.018) | 0.015 (0.013) | 0.014 (0.013) | 0.011 (0.009) | 0.010 (0.009) |
| Pop.($5d_{xy}$) | 1.938 (1.938) | 1.939 (1.939) | 1.939 (1.940) | 1.939 (1.939) | 1.931 (1.931) | 1.930 (1.931) | 1.824 (1.818) | 1.815 (1.817) |
| Pop.($5d_{xz}$) | 1.944 (1.944) | 1.944 (1.944) | 1.944 (1.945) | 1.944 (1.945) | 1.948 (1.948) | 1.948 (1.948) | 1.872 (1.868) | 1.866 (1.867) |
| Pop.($5d_{yz}$) | 1.957 (1.957) | 1.957 (1.957) | 1.957 (1.957) | 1.957 (1.957) | 1.948 (1.948) | 1.948 (1.948) | 1.875 (1.871) | 1.869 (1.871) |
| Pop.($5d_{x^2-y^2}$) | 0.970 (0.950) | 0.968 (0.949) | 0.940 (0.949) | 0.940 (0.951) | 0.889 (0.875) | 0.870 (0.881) | 1.297 (1.286) | 1.285 (1.287) |
| Pop.($5d_{z^2}$) | 1.799 (1.822) | 1.799 (1.823) | 1.828 (1.821) | 1.827 (1.821) | 1.779 (1.795) | 1.799 (1.791) | 1.846 (1.866) | 1.868 (1.866) |
| | Pd complex | | | | | | | |
| | **2a**, $PdCl_2(NH_3)$(glycine) | | | | **2b**, $[Pd(NH_3)_4]^{2+}$ | | **2c**, $[Pd(CN)_4]^{2-}$ | |
| Geom. | H-I | H-II | O-I | O-II | H-I | O-I | H-I | O-I |
| Pop.(5s) | 0.448 (0.426) | 0.448 (0.426) | 0.400 (0.420) | 0.404 (0.423) | 0.452 (0.432) | 0.417 (0.440) | 0.596 (0.583) | 0.568 (0.582) |
| Pop.($5p_z$) | 0.012 (0.009) | 0.012 (0.009) | 0.010 (0.009) | 0.009 (0.009) | 0.008 (0.006) | 0.007 (0.006) | 0.006 (0.004) | 0.005 (0.004) |
| Pop.($4d_{xy}$) | 1.962 (1.962) | 1.963 (1.963) | 1.964 (1.964) | 1.964 (1.964) | 1.958 (1.958) | 1.958 (1.958) | 1.886 (1.883) | 1.881 (1.883) |
| Pop.($4d_{xz}$) | 1.963 (1.963) | 1.963 (1.963) | 1.963 (1.963) | 1.963 (1.963) | 1.964 (1.965) | 1.965 (1.965) | 1.916 (1.914) | 1.912 (1.913) |
| Pop.($4d_{yz}$) | 1.970 (1.970) | 1.970 (1.970) | 1.971 (1.971) | 1.971 (1.971) | 1.964 (1.964) | 1.965 (1.965) | 1.917 (1.916) | 1.914 (1.916) |
| Pop.($4d_{x^2-y^2}$) | 1.020 (0.998) | 1.018 (0.996) | 0.973 (0.990) | 0.973 (0.991) | 0.938 (0.920) | 0.904 (0.923) | 1.351 (1.337) | 1.331 (1.336) |
| Pop.($4d_{z^2}$) | 1.895 (1.907) | 1.895 (1.907) | 1.912 (1.907) | 1.912 (1.907) | 1.887 (1.896) | 1.904 (1.896) | 1.902 (1.912) | 1.914 (1.913) |

[a]Calculated at the model geometry with three-regions 3D-RISM-MP2. Unit is in *e*. [b]In parentheses are calculated in the absence of the counterpart of the complex or **W** under the consideration of solvation around the super molecule, *i.e.* complex+**W**.

Table S6: Comparison of the solvation free energy between the 3D-RISM and PCM methods.[a]

| | Pt complex | | | | | | | |
|---|---|---|---|---|---|---|---|---|
| | **1a**, $PtCl_2(NH_3)$(glycine) | | | | **1b**, $[Pt(NH_3)_4]^{2+}$ | | **1c**, $[Pt(CN)_4]^{2-}$ | |
| Geom. | H-I | H-II | O-I | O-II | H-I | O-I | H-I | O-I |
| $\Delta\mu_{\mathrm{rism}}^{\mathrm{MP2}}$ | -13.5 | -12.5 | -14.7 | -16.4 | -177.4 | -159.3 | -178.2 | -188.5 |
| $\Delta\mu_{\mathrm{pcm1}}^{\mathrm{MP2}\,b}$ | (-5.0) | (-4.1) | (-2.4) | (-3.9) | (-184.9) | (-166.4) | (-152.5) | (-159.0) |
| $\Delta\mu_{\mathrm{pcm2}}^{\mathrm{MP2}\,c}$ | (-33.4) | (-32.1) | (-32.1) | (-32.6) | (-208.3) | (-190.9) | (-175.6) | (-183.5) |
| | Pd complex | | | | | | | |
| | **2a**, $PdCl_2(NH_3)$(glycine) | | | | **2b**, $[Pd(NH_3)_4]^{2+}$ | | **2c**, $[Pd(CN)_4]^{2-}$ | |
| Geom. | H-I | H-II | O-I | O-II | H-I | O-I | H-I | O-I |
| $\Delta\mu_{\mathrm{rism}}^{\mathrm{MP2}}$ | -14.0 | -12.6 | -15.5 | -17.3 | -175.6 | -157.1 | -178.3 | -189.6 |
| $\Delta\mu_{\mathrm{pcm1}}^{\mathrm{MP2}\,b}$ | (-6.2) | (-5.7) | (-4.3) | (-6.0) | (-184.0) | (167.2) | (-153.5) | (-160.9) |
| $\Delta\mu_{\mathrm{pcm2}}^{\mathrm{MP2}\,c}$ | (-34.7) | (-34.1) | (-33.1) | (-34.4) | (-207.7) | (-190.6) | (-176.7) | (-184.4) |

[a]Calculated at the model geometry with three-regions 3D-RISM-MP2. Unit is in kcal/mol. [b]Calculated by the PCM method with the ES and Cavity terms. [c]Calculated by the PCM method with only the ES term.

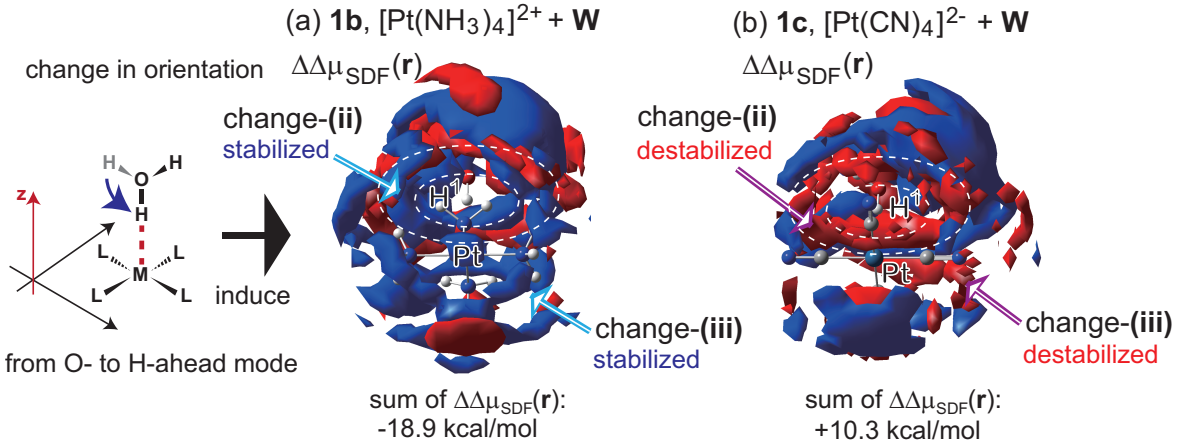


Figure S1: Bottom view of the change in spatial solvation free energy, $\Delta\Delta\mu_{\mathrm{SDF}}(\mathbf{r})$. Isovalues are the same as those in Figure 5.